STRUCTURAL
BIOLOGY

Volume 77 (2021)

Supporting information for article:

Neutralization of the anthrax toxin by antibody-mediated stapling of its membrane-penetrating loop

F. Hoelzgen, R. Zalk, R. Alcalay, S. Cohen-Schwartz, G. Garau, A. Shahar, O. Mazor and G. A. Frank

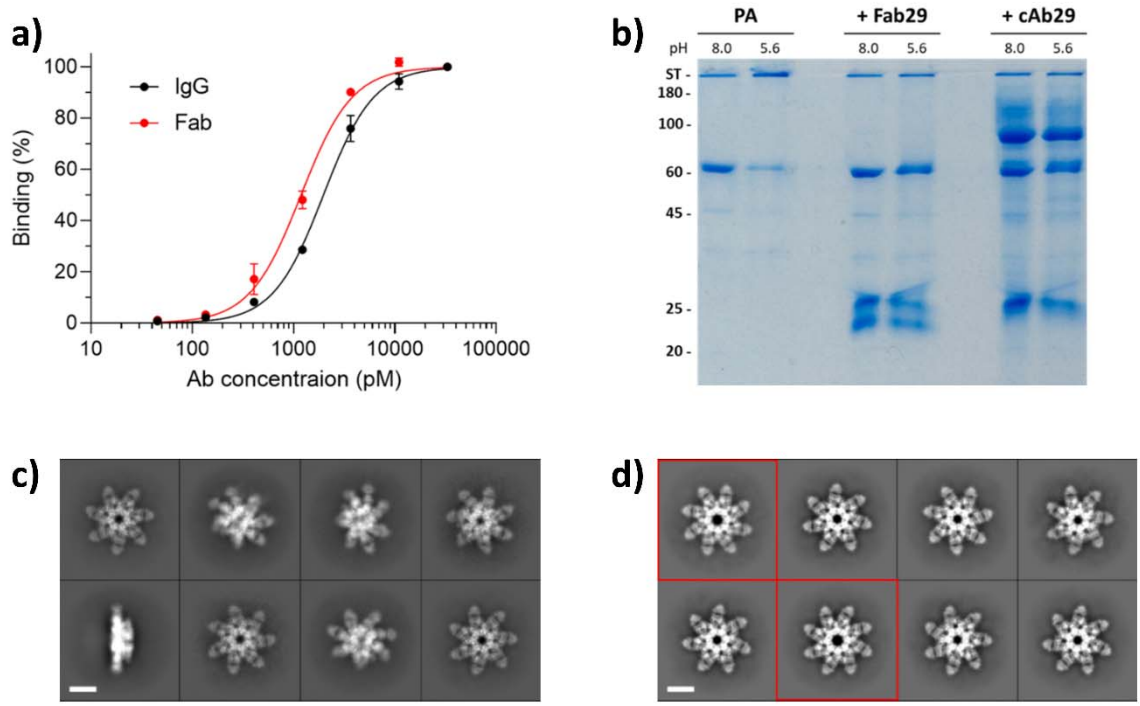

Figure S1 cAb29 and its Fab bind the prepore and block the prepare to pore transition. (a) Binding profiles of cAb29 antibody and cAb29-Fab tested by ELISA against PA. Values are averages of duplicates ± SEM, fitted by non-linear regression and expressed as percent of Bmax of each curve. The dissociation constants of the Fab and the antibody are 1.97±0.06 nM and 1.18±0.07 nM respectively. (b) Transition to the pore state was monitored by the formation of an SDS-resistant PA complex which did not migrate into the separating gel. The ability of PA to undergo the transition was tested by incubating PA, w/wo cAb29 or cAB29-Fab at a ratio of 9:7 Fab:PA-subunits, for 15 min, followed by an additional 15 min incubation at pH 5.6 (or pH 8.0, as a control), both incubations were done at room temperature. After incubation in low pH, SDS-PAGE samples were prepared by adding Laemmli buffer to the PA samples to a final concertation of 1x followed by incubation 10 minutes in room temperature prior to gel loading. Samples were resolved on 10% acrylamide gel. Samples' pH before addition of SDS is noted above the lanes. Only when the Fab and IgG are absent, treatment with low pH resulted in a decrease of the SDS sensitive phase manifested as a band expected of monomeric PA_{63} (2^{nd} lane, 63 kDa band). (c-d) Selected "good" 2D class averages form the dataset w/wo DDM (respectively). Class averages of top views of the octameric complex are highlighted by a red frame. Addition of DDM to the sample resulted in a broad orientation distribution of the PA-Fab complexes. Scale bar is 10 nm.

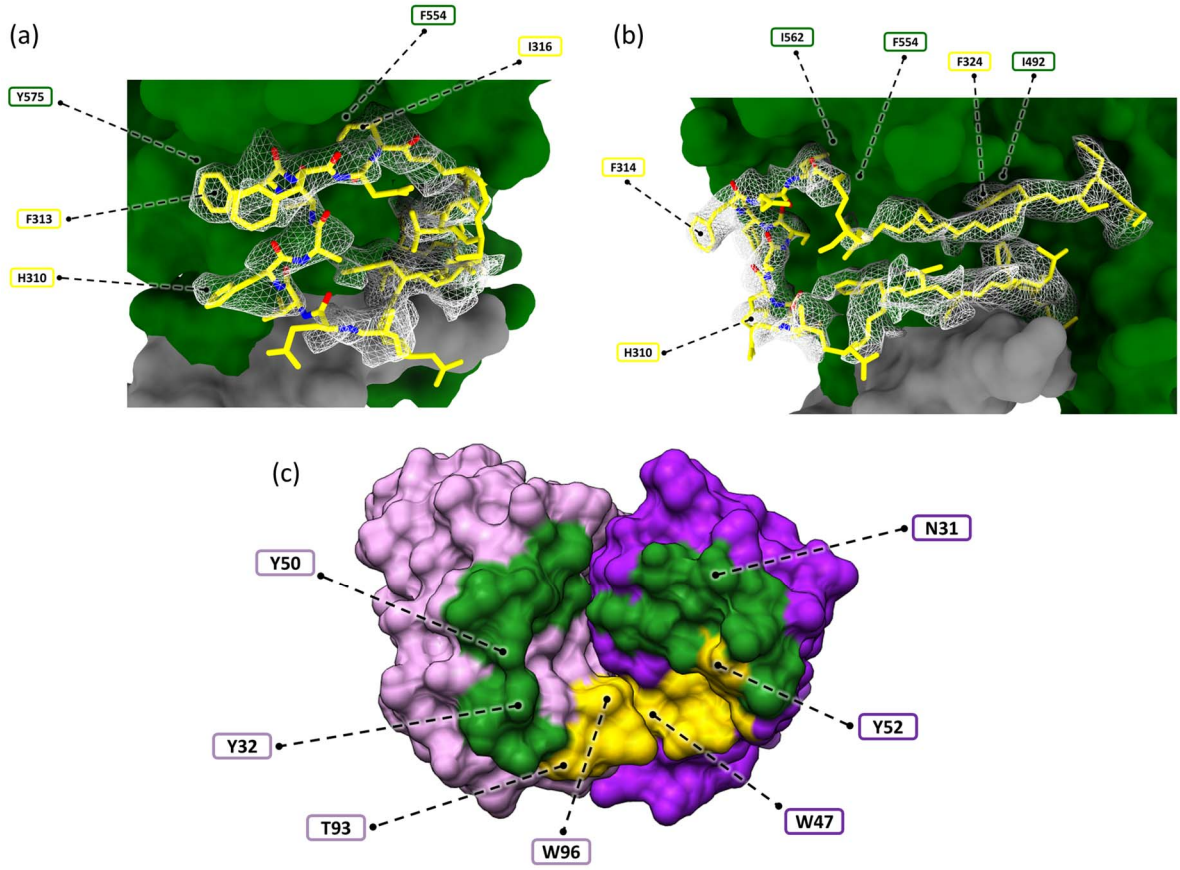

Figure S2 A closeup look at the three-dimensional architecture of the D2L2 loop, the D3 domain, and the Fab complex. (a-b) Organization of the D2L2 loop/D3 domain interface. The experimental electron density map of the D2L2 loop (white mesh) and the all-atom representation of its model (yellow) are viewed from the direction of the Fab inwards towards the center of the prepore ring in panel (a) and from the direction of the inter-subunit cleft in panel (b). The D3 and D4 domains are depicted as a flattened all-atom surface representation (green and gray respectively). The Fab and the neighboring subunits were removed to reveal these interfaces. (c) The footprint of the D2L2 loop and the D3 domain on the antigen-binding surface of cAb29. The light and heavy chains of cAb29 are colored light and dark purple, respectively. The surface of cAb29 that interacts with the D2L2 loop is colored yellow, and the surface that interacts with the D3 domain is colored green. The cAb29-Fab antigen-binding surface is viewed from the direction of the prepore ring outwards towards the Fab. The surface of the Fab is exposed by removing the PA. Some of the amino acids that contribute to the stability of the PA-cAb29 interface are designated (see figure 2b for a detailed interaction plot).

Table S1 List of amino acids forming the hydrophilic seal around the PA-Fab hydrophobic interface.

PA side	Fab side
T548, **D551**, N556, **N564**, **E568**, T572, N573, **T576**, K594, H597	Light chain: K92, **T93** Heavy chain: **N31**, N33, R54, T55, **D57**, S59, D99

*Amino acids depicted in figure 2b are in bold font.

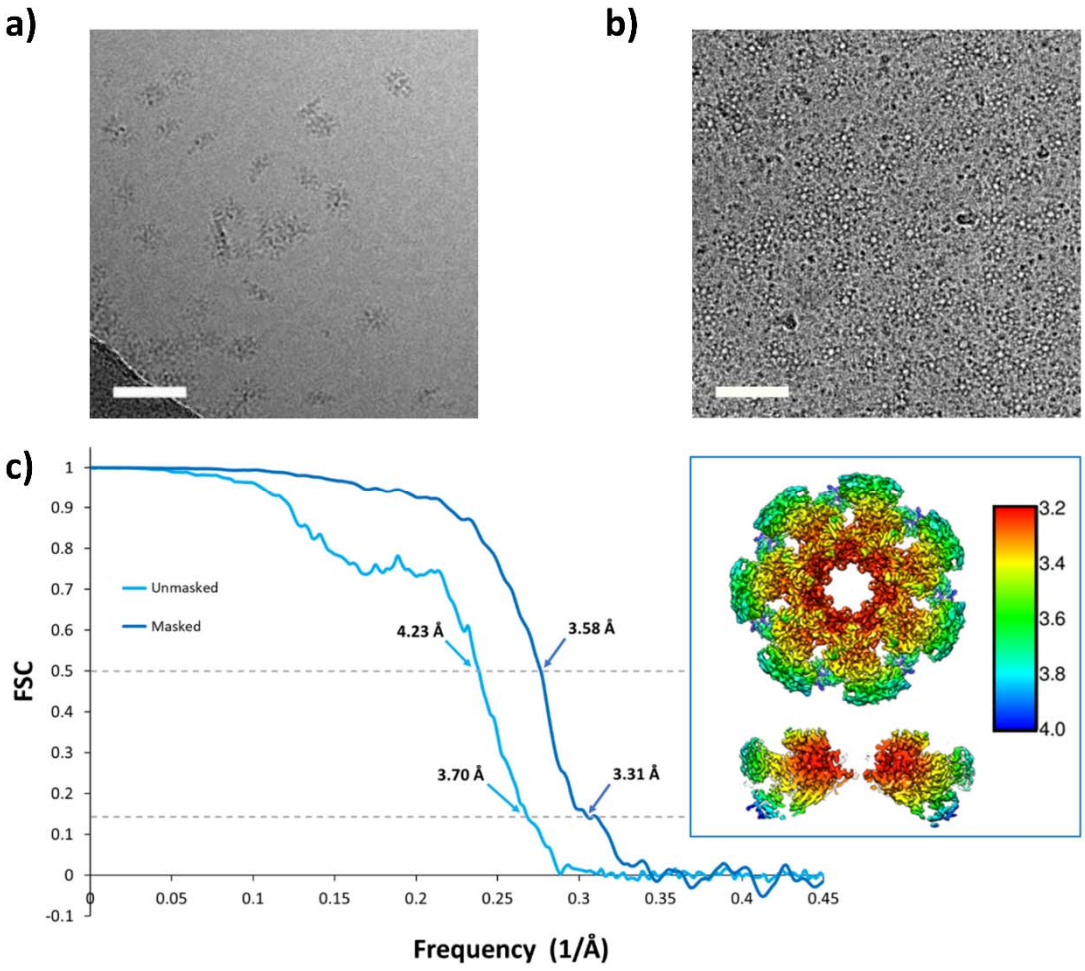

Figure S3 Summary of image processing of the cAb29-PA complex datasets. (a-b) Representative micrographs (cropped to ~0.25 field of view) of cAb29-PA complexes w/wo addition of 0.075 mM DDM (respectively). (c-d) Selected "good" 2D class averages form the dataset w/wo DDM (respectively). Class averages of top views of the octameric complex are highlighted by a red frame. Addition of DDM to the sample resulted in a broad orientation distribution of the PA-Fab complexes, however reduced the number of particles per field of view. (e) FSC plot of the resulting 3.3 Å map and the corresponding local resolution maps show a top overview of the structure and a slice through its center (inset). Scale bar is 50 nm.

Table S2 Data collection and refinement parameters of cryo-EM structures solved in this study.

PDB ID/EMDB Codes	7O85/EMD-12761
FSC(1/f)=0.143 Masked/Unmasked (Å)	3.5/3.9
FSC(1/f)=0.5 Masked/Unmasked (Å)	3.8/4.4
# of micrographs	6355
# of particles	211 K
Total dose (e-/Å2)	80
Pixel size (Å)	1.1
# of frames	50